β-actin mRNA interactome mapping by proximity biotinylation

Joyita Mukherjee[1], Orit Hermesh[1], Nicolas Nalpas[2], Mirita Franz-Wachtel[2], Boris Maček[2], Ralf-Peter Jansen[1,3]

1 Interfaculty Institute of Biochemistry, University of Tübingen, Tübingen, Germany.

2 Proteome Center Tübingen, University of Tübingen, Tübingen, Germany.

3 Corresponding author: Ralf-Peter Jansen
University of Tübingen
Interfaculty Institute of Biochemistry
Hoppe-Seyler-Strasse 4
72076 Tübingen, Germany
Phone: +49-7071-2974161
Email: ralf.jansen@uni-tuebingen.de

KEYWORDS:

RNA-BioID, mRNA localization, FUBP3, RNA binding protein, protein−RNA interaction, object-based co-localization

RUNNING TITLE:

RNA-BioID identifies β-actin mRNA-associated proteins

ABSTRACT

Function and fate of mRNAs are controlled by RNA binding proteins (RBPs) but determining the proteome of a specific mRNA *in vivo* is still challenging. RNA proximity biotinylation on the transported β-actin mRNA tagged with MS2 aptamers (RNA-BioID) is used to characterize the dynamic proteome of the β-actin mRNP in mouse embryonic fibroblasts (MEFs). We have identified > 60 β-actin associated RBPs including all six previously known as well as novel interactors. By investigating the dynamics of the β-actin mRNP in MEFs, we expand the set of β-actin mRNA associated RBPs and characterize the changes of the interacting proteome upon serum-induced mRNA localization. We report that the KH-domain containing protein FUBP3 represents a new β-actin associated RBP that binds to its 3'-untranslated region outside the known RNA localization element but is required for β-actin RNA localization. RNA-BioID will allow obtaining a dynamic view on the composition of endogenous mRNPs.

INTRODUCTION

The spatial distribution of mRNAs contributes to the compartmentalized organization of the cell and is required for maintaining cellular asymmetry, proper embryonic development and neuronal function[1]. Localized mRNAs contain cis-acting regions, termed zipcodes or localization elements that constitute binding sites for RNA-binding proteins (RBPs)[2]. Together with these RBPs, localized mRNAs form transport complexes containing molecular motors such as kinesin, dynein, or myosin[3,4]. These ribonucleoprotein complexes (RNPs) usually include accessory factors such as helicases, translational repressors, RNA stability factors or ribosomal proteins[5]. Thus, mRNPs as functional units do not only contain the information for an encoded polypeptide but also determine the precise spatio-temporal regulation of its translation, thereby facilitating the correct subcellular localization of the translation product[6]. One of the best-studied localized mRNAs is β-actin that encodes the β isoform of the cytoskeleton protein actin[7,8,9]. β-actin mRNA is localized to the leading edge of migrating fibroblasts[10] where its local translation critically contributes to the migrating behavior of this cell type[7]. In mouse[10] and *Xenopus*[11] neurons, β-actin mRNA is transported to the growth cone during axonal extension and its deposition and local translation is highly regulated by external cues. In addition, translation of this mRNA in dendritic spines is involved in re-shaping the postsynaptic site of synapses[12]. A well-defined localization element is located in the proximal region of the β-actin 3'

untranslated region (3'-UTR)[13]. This cis-acting signal is recognized by the zipcode-binding protein ZBP1[14], an RBP of the conserved VICKZ RNA-binding protein family[15]. ZBP1 (also called IGF2BP1 or IMP1) interacts with the zipcode via two K-homology (KH) RNA-binding domains and is required for RNA localization in fibroblasts and neurons[16]. In addition, it controls translation of β-actin by blocking the assembly of ribosomes at the start codon[17]. IGF2BP1 appears to act as key RBP in β-actin mRNA distribution but several other proteins have been involved in β-actin mRNA localization, although their molecular function is less clear.

To fully understand mRNA localization and its regulation, it is important to know the proteins binding and controlling these mRNAs. Major technological advances like CLIP (crosslinking and immunoprecipitation) combined with next-generation sequencing allow the identification of RNAs bound to specific RBPs[18,19] or the system-wide identification of RBPs that bind to polyA RNA[20,21]. However, the major approaches to determine which proteins associate with a specific RNA have been affinity purification of modified or tagged RNAs together with their bound proteins, or co-immunoprecipitation of RNP components with the help of known RNA-specific RBPs. In addition, affinity capturing of specific RNPs with hybridizing antisense probes has been successfully used[22,23,24]. A serious limitation of these techniques is the potential loss of low affinity binders during purification, which has so far been addressed by *in vivo* UV cross-linking prior to cell lysis. However, cross-linking enhances only the recovery of RBPs directly contacting nucleobases and therefore does not overcome the loss of other physiologically important RNA interactors, e.g. motor or adapter proteins. These limitations could be overcome by *in vivo* labelling of proteins while they are associated with the target RNA. BioID[25] has been successfully used to detect subunits of large and dynamic protein complexes like the nuclear pore complex[26] or centrosome[27]. In BioID, a protein of interest is fused to a mutant version of the *E. coli* biotin ligase BirA (BirA*) that generates AMP-biotin ('activated biotin'), which reacts with accessible lysine residues in its vicinity[28]. After lysis, biotinylated proteins can be isolated via streptavidin affinity purification and identified using standard mass spectrometry techniques. Recently, BioID has also been applied to identify proteins associated with the genomic RNA of ZIKA virus[29]. We have adapted it to characterize the proteome of an endogenous, localized β-actin mRNP. We report here that tethering of BirA* to an endogenous transcript does not only allow the identification of its associated proteins but can also be used to probe the environment of this mRNA. This approach allows, with high confidence, to identify novel

functional β-actin interactors that are as highly enriched as already reported β-actin interacting proteins IGF2BP1, IGF2BP2[30], RACK1[31], KHSRP[32], KHDBRS1/Sam68[33,34], and FMR1[35,36]. This is exemplified by FUBP3/MARTA2, an RBP from the conserved FUBP family of proteins[37,38] which was previously shown to mediate dendritic targeting of MAP2 mRNA in neurons[39,40] but is shown here to bind to and facilitate localization of β-actin mRNA to fibroblast protrusions. FUBP3 does not bind to the zipcode or IGF2BP1 and mediates β-actin RNA localization by binding to its 3'-UTR.

RESULTS

Tethering a biotin ligase to the 3'-UTR of β-actin mRNA

To tether BirA* to the 3'-UTR of β-actin mRNA (Figure 1a), we stably expressed a fusion of the MS2 coat protein (MCP)[41], eGFP and BirA* (MCP-eGFP-BirA*) in immortalized mouse embryonic fibroblasts (MEFs) from transgenic β-actin-MBS mice[42]. These mice have both β-actin gene copies replaced by β-actin with 24 MS2 binding sites (MBS) in their distal 3'-UTR. In addition, MCP-eGFP-BirA* or MCP-eGFP was also stably expressed in control MEFs with untagged β-actin. Co-expression of MCP-eGFP[42] or MCP-eGFP-BirA* (Supplementary Figure S1) does not affect β-actin mRNA and protein levels. Proximity labeling was performed by addition of 50 µM biotin to the medium at least for 6 hrs[28]. In cells expressing β-actin-MBS / MCP-eGFP-BirA* but not in control cells expressing only MCP-eGFP (Figure 1a) we observed biotinylation of numerous proteins in addition to the endogenous biotinylated proteins seen in cultured cells[25] (Figure 1). To test if proximity labeling can identify known β-actin mRNA-associated proteins, we affinity purified biotinylated proteins followed by Western Blot detection of IGF2BP1 (mouse ZBP1). IGF2BP1 was biotinylated in MEFs expressing MCP-eGFP-BirA* but not in those expressing MCP-eGFP-BirA* (Figure 1b) which demonstrates that our tool can successfully biotinylate zipcode interacting protein. Since biotinylation or the expression of the MCP-eGFP-BirA* might affect localization of the β-actin mRNA, we also checked proper targeting of β-actin mRNA to cell protrusions. To induce localization, MEFs expressing or non-expressing the biotin ligase-containing fusion protein were serum starved for 24 hrs and stimulated for 2 hrs[7,10]. In both MEF lines, we observed formation of motile cytoplasmic mRNPs and their targeting to cell protrusions (Figure 1c). We expected that a major fraction of biotinylated proteins is MCP-eGFP-BirA* itself. We therefore aimed at depleting the fusion protein from the lysate by GFP pulldown prior to streptavidin affinity purification. Surprisingly, most of the biotinylated proteins were enriched in the GFP pulldown

fraction (Figure 1d, lane 2), which is likely due to co-purification of MCP-eGFP-BirA*, β-actin mRNA and biotinylated proteins binding to the mRNA or the fusion protein. RNA degradation with RNase A (Supplementary Figure S2) shifted a large part of the biotinylated proteins into the streptavidin fraction (Figure 1d, lane 8), supporting the idea that most of the biotinylated proteins are associated with β-actin mRNA. Additional treatment with high salt and 0.5% SDS further optimized the streptavidin affinity purification and decreased the background binding of the magnetic beads used in this purifcation (Figure 1d, lane 12).

β-actin mRNA interactors under serum-induced and uninduced conditions

β-actin mRNA localization to the lamellipodia of chicken and mouse fibroblasts increases after serum induction[43]. It was also shown that during serum starvation, cells enter a quiescent phase of the cell cycle[44] with an overall reduction in actin stress fibers or focal adhesions[43]. Since efficient biotinylation and capturing requires 6 hrs of incubation with biotin, we next applied smFISH to verify that β-actin mRNA localization persists during our labeling period. As shown before[42], mouse fibroblasts induce β-actin mRNA localization after serum addition (Supplementary Figure S3a) and the fraction of MEFs with β-actin localized to lamellipodia increases within one hour but remains constant over the next 6 hours (Supplementary Figure S3b). This situation gives us an opportunity to biotinylate proteins that are associated with localizing β-actin mRNA during the required 6-hour labelling window.

To determine and compare the β-actin associated proteomes in uninduced and serum-induced MEFs, we performed RNA-BioID under both conditions (three replicate experiments each). Unspecific as well as endogenous biotinylation was assessed by performing BioID in MEFs expressing NLS-MCP-eGFP-BirA* in the absence of MS2 aptamers. Affinity-captured biotinylated proteins were identified and quantified by mass spectrometry using label free quantification (LFQ; see Methods). Principal component analysis of the datasets revealed that the different conditions cluster apart from each other in dimensions 1 and 2 (explaining 33.8% and 15.5% of variance), while the replicates within the same condition cluster together showing good biological reproducibility (Supplementary Figure S4). We furthermore calculated the Spearman correlation between all sample types and replicates, which demonstrates the high reproducibility between biological replicates (correlation ≥ 0.97). In addition, it showed better correlation between uninduced and induced samples (average 0.95) compared to control (Supplementary Figure S5). In total, there were 169 (or 156) significantly enriched proteins in

induced (or uninduced) MEFs compared to control cells (Supplementary Figure S6). Of these, 47 were enriched only under induced conditions (Supplementary table 4). To assess the differential enrichment of the proteins under each condition, a Tukey post-hoc test was performed after the ANOVA, and the significance was set to an adjusted p-value of 0.05 following Benjamini-Hochberg multiple correction testing (see Materials and Methods). A large fraction of the enriched proteins (30% and 34%) under induced, or uninduced conditions respectively, represent RNA-binding proteins (Figure 2, red solid circles). Among these are the majority of RBPs (IGF2BP1, IGF2BP2, KHSRP, KHDRBS1, FMR1, HuR[45], RACK1) already known to control specific aspects of β-actin mRNA physiology. Other enriched RBPs have been associated with the localization of mRNAs in other cell types or organisms, including STAU1 and STAU2[46], SYNCRIP[47], and FUBP3[48]. Furthermore, 85 proteins were significantly enriched under serum-induced compared to uninduced conditions (Supplementary figure S6). However, the majority of the above mentioned RBPs (including IGF2BP1) become biotinylated under induced as well as uninduced conditions, indicating that they are associated with β-actin mRNA under both conditions (Figure 2c).

A cluster analysis (Figure 3) reveals at least five different patterns of biotinylated proteins in induced, non-induced and control MEFs (Figure 3b, c). In control MEFs, we see enrichment of mainly nuclear proteins (cluster 1). This is expected since the unbound MCP-eGFP-BirA* is enriched in the nucleus due to an N terminal nuclear localization sequence[49] (Figure 1c). Cluster 1 also contains abundant cytoplasmic proteins like glycerol aldehyde phosphate dehydrogenase (GAPDH). Cluster 3 represents proteins that are equally found in MEFs under all conditions and contains e.g. ribosomal proteins. Proteins allocated to the other three clusters (clusters 2, 4, 5) are overrepresented in the biotinylated proteome of MEFs expressing β-actin-MBS. Of specific interest are clusters 4 and 5. In cluster 4, with proteins that are more biotinylated under serum-induced conditions, we find RNA-binding proteins, among them FMR1 and KHSRP[32] that have been reported to function in β-actin mRNA localization or bind to IGF2BP1. Another group of proteins that are enriched in this cluster are proteins of the actin cytoskeleton (e.g. Filamin B, Cofilin-1, Myh9, Tpm4, Plastin-3). Their enrichment likely reflects the deposition of the β-actin mRNA in the actin-rich cortical environment of the MEF's leading edge. Finally, cluster 5 contains proteins found in β-actin-MBS MEFs under induced as well as non-induced conditions but not in control MEFs. This cluster shows an enrichment for proteins involved in mRNA-binding, RNP constituents or ribosomal proteins. Since this cluster contains the zipcode-binding

protein IGF2BP1, we hypothesized that other proteins in this cluster, e.g. FUBP3 are likely candidates for β-actin mRNA regulatory factors.

FUBP3 is a component of the β-actin mRNP

To confirm the association of FUBP3 and MS2-tagged β-actin mRNA, we transfected MEFs expressing β-actin-MBS/MCP-GFP cells with plasmids encoding either FUBP3-mCherry or IGF2BP1-mCherry (Supplementary Figure S8a). An object based colocalization analysis of snapshot images was used to determine the extent of colocalization of each of the two proteins with β-actin mRNA[50]. For comparison of colocalization levels, a clipping point was chosen as the midway between zero distance and the onset of the random dominated colocalization (the plateau), represented also as the pick in the derivative graph which in our case was at 150 nm (Supplementary figure S8b-d). The colocalization of β-actin-MBS mRNA with each protein at this clipping point distance was small but significant with 6.6 ± 4.1% for IGF2BP1 and 4.4 ± 6.2% for FUBP3 (Supplementary figure S8e). To test if the observed colocalization of the mCherry fusion proteins is in the range of the endogenous proteins, we combined single-molecule FISH (smFISH) against β-actin-MBS and immunofluorescence (smFISH-IF) using antibodies against FUBP3 and IGF2BP1 (Figure 4a). We also included IGF2BP2 in this analysis since it has been suggested to interact with IGF2BP1 and β-actin mRNA[30] and was found in our analysis in the same cluster as IGF2BP1 and FUBP3 (Figures 2 and 3). smFISH with probes against the β-actin ORF and the MBS part allowed us to estimate the feasibility of our method to detect colocalization (Figure 4a). 5.8% of β-actin mRNA signals co-localize with FUBP3, 4% co-localize with IGF2BP2 and 10.3% co-localize with IGF2BP1 (Figure 4c, supplementary figure S9). Applying the same colocalization to β-actin ORF and the MBS part, 31% of MS2 probes were found to colocalize with β-actin ORF. This indicates that our colocalization analysis likely underestimates the degree of true colocalization by a factor of three. One of the reasons for this low number could be the high number and crowdedness of distributed signals in case of β-actin mRNPs resulting in an increase in random estimated colocalization values that were used to evaluate true colocalization. Furthermore, our setup lacked the high-level correction for chromatic and mechanical microscope aberration that was shown to be beneficial for the correct quantification of these interactions[51]. The quantitative analysis of colocalization between β-actin and FUBP3, although being in the same range of IGF2BP1 (6-10 %), is still lower than expected. Aside from the technical reasons, the low value

could be due to the use of immortalized MEFs. In contrast to primary MEFs, immortalized MEFs have a lower efficiency of β-actin localization, which is likely due to increased phosphorylation of IGF2BP1 and its release from the zipcode[52,50]. Alternatively, the low degree of colocalization could be due to the dynamic interaction of FUBP3 and IGF2BP1 with the β-actin mRNP[53]. Analyzing snap shots of this interaction could therefore also result in an underestimation of the RBP's association with β-actin mRNA as it was shown in the case of kinesin-1 interaction with oskar mRNA in *Drosophila* oocytes[50].

FUBP3 binds to the 3'-UTR of β-actin mRNA

To validate our colocalization experiments, we performed co-immunoprecipitation of β-actin mRNA with FUBP3 and IGF2BP1 (Figure 5a). Both proteins co-precipitate four tested mRNAs (β-actin, Cofilin1, Igf2bp1, Fubp3). In case of IGF2BP1, it binds to all the mRNAs tested, which reflects previous observations in Hela cells, where almost 3% of the transcriptome was shown to bind to IGF2BP1[54]. β-actin binding to FUBP3 (23% of input bound to FUBP3) was less efficient than to IGF2BP1 (37%) (which also correlates with the microscopy results). We also detected FUBP3 and IGF2BP1 binding to another localized mRNA, Cof1[55] to a similar extent (48%). Since co-precipitation of these mRNAs with FUBP3 could be indirect, e.g. via IGF2BP1, we used recombinant glutathione S transferase (GST)-FUBP3 and IGF2BP1 (Supplementary figure S10) in pulldown assays to test direct binding to *in vitro* transcribed RNA fragments of β-actin mRNA. We selected the 54 nucleotide localization zipcode element of β-actin, a 49 nucleotide long region after the zipcode (proximal zipcode)[14] and the 643bp long whole β-actin 3'-UTR. RNA captured by the GST fusion proteins was detected by quantitative RT-PCR and normalized to the input. As negative controls, GST protein and a zipcode mutant RNA unable to bind to IGF2BP1[56,57] were used. Unlike IGF2BP1, FUBP3 does not bind to the zipcode but does interact with the 3'UTR of β-actin mRNA, suggesting that it recognizes a different site in the 3'-UTR (Figure 5b). A recent publication[58] revealed that FUBP3 binds the motif UAUA, which is also present at the 3'UTR of β-actin mRNA, 459bp downstream of the stop codon. To further substantiate our finding that FUBP3 can bind independently of IGF2BP1 to β-actin mRNA, we performed co-immunoprecipitation experiments of IGF2BP1 and FUBP3 (Figure 5c). We did not detect co-immunoprecipitation of IGF2BP1 and FUBP3. However, as reported[59], we see that IGF2BP2 binds to IGF2BP1, indicating physical interaction between these two proteins. We conclude that FUBP3 does not directly bind to IGF2BP1.

To identify the KH domain of FUBP3 responsible for interaction with β-actin mRNA, we introduced mutations in the conserved KH domains of the protein. Each functionally important G-X-X-G motif in the four KH domains was changed to an inactive version (G-D-D-G)[60] and individual mutant proteins were transiently expressed in MEFs as C-terminally tagged mCherry fusion protein. The G-D-D-G mutation in KH domain KH2 resulted in loss of the cytoplasmic punctate staining seen in wild type FUBP3, which is reminiscent of a similar punctate pattern observed for mRNPs (Figure 5d). We conclude that KH2 in FUBP3 is important for its integration into RNP particles and likely constitutes the critical domain for RNA binding.

Loss of FUBP3 affects β-actin mRNA localization

To validate that proteins identified by RNA-BioID are functionally significant for the mRNA used as bait, we performed knockdown experiments for Fubp3. Knockdown of Igf2bp1 was used as a positive control for a factor involved in β-actin localization. The knockdown effectiveness was validated by western blot against IGF2BP1 and FUBP3, using GAPDH and β-ACTIN as controls (Figure 6a, b, and Supplementary figure S11). The effect of the knockdown on β-actin mRNA localization was assessed by smFISH (Figure 6c and supplementary figure S12). In control cells, up to 47% of MEFs show localized β -actin mRNA in their protrusions (Figure 6c). IGF2BP1 knockdown reduces this to 32% while FUBP3 knockdown leads to a reduction to 21% (Figure 6c). This indicates that FUBP3 is important for β-actin mRNA localization. In addition, we found that knockdown of Igf2bp1 or Fubp3 only mildly changes β-actin mRNA levels (79% of wild type in case of Igf2bp1 knockdown, 93% in case of Fubp3). In contrast, the level of β-actin protein increases to 120%, or 150%, respectively (Figure 6a, b). In case of IGF2BP1, this is consistent with previous reports showing that the protein acts as translational repressor of β-actin mRNA and that localization defects seen after loss of IGF2BP1 are due to premature translation of the mRNA before reaching its normal destination site[17,61]. FUBP3 could perform a similar role on β-actin mRNA.

DISCUSSION

Proximity biotinylation has facilitated the characterization of dynamic protein complexes by *in vivo* labeling of interaction partners. Here, we exploit this approach and demonstrate its utility for identifying functionally relevant RNA-binding proteins of a specific mRNA, mammalian β-actin. This is

achieved by combining MS2 tagging of the mRNA of choice and co-expression of a fusion protein of the MS2 coat proteins (MCP) and the biotin ligase (BirA*).

The primary goal for an RNA-based BioID is the identification of novel RNA interactors. As seen before in several proximity labeling (BioID or APEX-driven) approaches[62,63,64], the number of identified potential interactors for β-actin is far higher than the number of proteins identified in classical co-immunoprecipitation or co-affinity purification approaches. This might be due to the higher sensitivity of proximity labeling or its propensity to allow capturing of transient interactors[62]. Although this can results in a skewed view of the actual components of a complex due to the rapid change of the composition of mRNP, it is beneficial in order to identify all the mRNP components during the life stages of an mRNA. The most highly represented class of proteins were RBPs (Figure 3 and S7b), among them all RBPs that have been previously associated with localization, translational control or (de)stabilization of β-actin mRNA. Other RBPs like survival of motor neuron 1 (SMN1), which supports the association of IGF2BP1 with β-actin mRNA[65,66], were also found to be enriched in MEFs expressing β-actin-MBS compared to control MEFs, although with lower significance (p-value < 0.1). We also analyzed our dataset for motor proteins involved in mRNA transport. Neither MYH10[67] nor KIF11[68] that have been suggested to work as β-actin mRNA transport motors were found as biotinylated proteins. In contrast, the only motor we identified is MYH9, the heavy chain of a MYH10 related class II-A myosin although it was not significantly enriched ($p = 0.08$). The lack of motor proteins is compatible with a recent observation that β-actin localization in fibroblasts works primarily by diffusion to and trapping in the microfilament-rich cortex[42]. This is also corroborated by our finding that components of the actin-rich cell protrusion (Figure 3, cluster 4) are heavily biotinylated in MEFs after serum-induced localization of β-actin.

Overall, the cluster analysis shows that the majority of previously identified β-actin RBPs behave similarly under the two tested conditions (serum-induced and uninduced MEFs). This not only indicates that they interact with β-actin mRNA in MEFs even under steady state conditions, but It also makes it likely that other proteins, especially RBPs, found in this cluster might represent so far unknown β-actin mRNA interactors. By choosing the far-upstream binding protein FUBP3 as a potential candidate we demonstrate that this assumption holds true for at least this protein. FUBP3 not only binds to β-actin mRNA but its knockdown also results in a similar decrease of β-actin localization to the leading edge as seen for loss of IGF2BP1.

FUBP3, also named MARTA2 has been reported to bind to the 3'-UTR of the localized MAP2 mRNA in rat neurons[40] and regulates its dendritic targeting[48]. Although the binding site of FUBP3 in MAP2 mRNA is not known, its preferred binding motif (UAUA) was recently identified[58]. This motif is present in the 3'-UTR of β-actin 405 bp downstream of the zipcode. FUBP proteins might play a more substantial role in RNA localization since homologs of a second member of the FUBP family, FUBP2 were not only reported to be involved in MAP2 or β-actin mRNA localization[48,32] but also present among the biotinylated proteins we identified. However, FUBP2 is mainly nuclear and its role in β-actin mRNA localization might be indirect[32]. In contrast, FUBP3 seems to have a direct function in localizing β-actin. Although we observed only little colocalization of β-actin mRNPs and FUBP3, colocalization was in the range of that seen for IGF2BP1. More important, FUBP3 binds to the 3'-UTR and its loss reduces β-actin mRNA localization. FUBP3 and IGF2BP1 do not bind directly to each other. Finally, IGF2BP1 levels are not affected by Fubp3 knockdown, ruling out an indirect effect on β-actin mRNA localization via changing IGF2BP1 amounts. What might therefore be the function of FUBP3? A potential function could be translational regulation. Similar to Igf2bp1 knockdown, loss of FUBP3 results in increased amounts of β-actin protein while β-actin mRNA levels are similar to or even lower than in untreated MEFs. This could be due to a loss of translational inhibition as it has been shown for IGF2BP1.

Its role in β-actin and MAP2 mRNA localization suggests that FUBP3/MARTA2 is a component of several localizing mRNPs. Of note, RNA-BioID on β-actin mRNA has identified even more RBPs that have been previously involved in the localization of other mRNAs, e.g. SYNCRIP[69] or Staufen[46]. Several of these like STAU1 and STAU2 are highly enriched in our β-actin biotinylated proteome. This finding might on one hand reflect the participation of multiple RBPs in β-actin localization or regulation. It also shows that a common set of RBPs is used to control the fate of several different localized mRNAs in different cell types. Although RNA-BioID does not currently allow us to determine if all these RBPs are constituents of the same β-actin mRNP, belong to different states of an mRNP or to different populations, their identification now allows addressing these questions to reach a more detailed understanding of the common function of RBPs on diverse mRNAs.

MATERIALS AND METHODS

Cell culture methods as well as general molecular and cell biology techniques including plasmid cloning, lentiviral transfection and selection, immunoprecipitation and western blotting, and *in situ* hybridization are described in Supplementary Methods.

RNA-BioID: For RNA-BioID, cells were incubated with 50 µM biotin at least for 6 hrs. Following incubation, cells were washed twice with 1x PBS and lysed in IP lysis buffer (50 mM Tris pH 7.5, 150 mM NaCl, 2.5 mM $MgCl_2$, 1 mM DTT, 1% tween-20, and 1x proteinase inhibitor) and passed 10-12 times through a 21G needle. The lysate was cleared by centrifugation (12,000 x g for 10 min at 4°C) to remove cell debris. 10 µg of protein from the supernatant ('total cell lysate') were used to check for protein biotinylation. In the remaining lysate, NaCl was added to a final concentration of 500 mM. 200 µl of a streptavidin magnetic bead suspension (GE Healthcare) were added and the high salt lysate incubated overnight at 4°C with end to end rotation. On the next day, the beads were collected (by keeping the beads on the magnetic stand for 2 min) and washed as described before[28]. In detail, they were washed twice for 5 min with 0.3 ml wash buffer 1 (2% SDS), once with wash buffer 2 (0.1% (w/v) deoxycholate, 1% (w/v) tween-20, 350 mM NaCl, 1 mM EDTA pH 8.0), once with wash buffer 3 (0.5% (w/v) deoxycholate 0.5% (w/v) tween-20, 1 mM EDTA, 250 mM LiCl, 10 mM Tris-HCl pH 7.4) and 50 mM Tris-HCl pH 7.5, once with wash buffer 4 (50 mM NaCl and 50 mM Tris-HCl pH 7.4), and finally twice with 500 µl of 50 mM ammonium bicarbonate. 20 µl of the beads were used for western blot and silver staining, and 180 µl was subjected to mass spectrometry analysis. To release captured proteins for western blot analysis from streptavidin beads, the beads were incubated in 2x Laemmli buffer containing 2 mM saturated biotin and 20 mM DTT for 10 min at 95 degree.

For biotinylation after serum induction, cells were starved for 24 hrs as described in supplementary methods and induced with 10% serum containing media containing 50 µM biotin for at least for 6 hrs to 24 hrs. Samples were processed for mass spectrometric analysis as described in Supplementary Methods.

Microscopy and object-based colocalization analysis: Cells were imaged with a Zeiss CellObserver fluorescence microscope equipped with a CCD camera (Axiocam 506) and operated by ZEN software (Zeiss). Image stacks were taken at 26-micron distance with either 40x,63x or 100x 1.4

NA oil immersion objectives. A representative slice was subjected to image processing and object-based localization. Particles were identified using the mexican hat filter plug-in available for Fiji which apply Laplacian of Gaussian filter to a 2D image. Object based localization was performed using the xsColoc imageJ plugin as described[70]. Briefly, the plugin determines the colocalization of objects in single snapshot frames by measuring the distance between closest neighbor objects from the β-actin mRNP (reference channel) and the protein (target channel). The analysis was restricted to the cytoplasm. Random colocalization was addressed by seeding objects from the target channel randomly into the defined area (cytoplasm), a process that was repeated 100 times. Particles from the reference channel were randomly assigned to clusters in the size of 100 particles. The fraction of colocalization as a function of maximal localization distance in each cluster was compared to the distribution of 100 simulated random values using the one sample student's t-test (α=0.01). The difference between the significant clusters to the random value was used in order to detect the 'real' co-localization[32].Extraction, statistical analysis and plotting of the data produced by the xsColoc plugin were carried out in R using the R Studio front-end (https://www.rstudio.com/) and the ggplot2 library[71] to plot the graphs. The R script to analyze the data was written and kindly provided by Imre Gaspar.

Data availability: Proteomic data supporting this study has been deposited into PRIDE, accession no: PXD010694.

Author Contributions: JM and RPJ conceived the project. JM and OH performed experiments, analyzed the data and wrote the manuscript. MFW, NN, JM, and BM designed, performed and analyzed the mass spectrometry experiments. RPJ supervised the project, interpreted the data and wrote the manuscript.

Acknowledgement: We thank Jeff Chao (FMI, Basel), Imre Gaspar (EMBL, Heidelberg), Julién Bethune (BZH, Heidelberg), Stefan Kindler (U. Hamburg), Stefan Hüttelmaier (U. Halle), and Ibrahim Muhammad Syed (IFIB, U. Tübingen) for plasmids, cell lines, antibodies, or spike RNA. We are grateful to Frank Essmann (IFIB, U. Tübingen) and Silke Wahle (PCT, U. Tübingen), for technical support and Matthew Cheng (IFIB, U. Tübingen) for suggestions on the manuscript. The project was funded by the Deutsche Forschungsgemeinschaft (DFG-FOR2333).

REFERENCES:

1. Martin, K. C. & Ephrussi, A. mRNA localization: gene expression in the spatial dimension. *Cell* **136,** 719–30 (2009).

2. Buxbaum, A. R., Haimovich, G. & Singer, R. H. In the right place at the right time: visualizing and understanding mRNA localization. *Nat. Rev. Mol. Cell Biol.* **16,** 95–109 (2015).

3. Eliscovich, C., Buxbaum, A. R., Katz, Z. B. & Singer, R. H. mRNA on the move: the road to its biological destiny. *J. Biol. Chem.* **288,** 20361–8 (2013).

4. Bullock, S. L. Messengers, motors and mysteries: sorting of eukaryotic mRNAs by cytoskeletal transport: Figure 1. *Biochem. Soc. Trans.* **39,** 1161–1165 (2011).

5. Marchand, V., Gaspar, I. & Ephrussi, A. An Intracellular Transmission Control Protocol: Assembly and transport of ribonucleoprotein complexes. *Current Opinion in Cell Biology* (2012). doi:10.1016/j.ceb.2011.12.014

6. Dreyfuss, G., Kim, V. N. & Kataoka, N. MESSENGER-RNA-BINDING PROTEINS AND THE MESSAGES THEY CARRY. *Nat. Rev. Mol. Cell Biol.* **3,** 195–205 (2002).

7. Kislauskis, E. H., Zhu, X. & Singer, R. H. beta-Actin messenger RNA localization and protein synthesis augment cell motility. *J. Cell Biol.* **136,** 1263–70 (1997).

8. Condeelis, J. & Singer, R. H. How and why does beta-actin mRNA target? *Biol. Cell* **97,** 97–110 (2005).

9. Bunnell, T. M., Burbach, B. J., Shimizu, Y. & Ervasti, J. M. Beta-Actin specifically controls cell growth, migration, and the G-actin pool. *Mol. Biol. Cell* **22,** 4047–4058 (2011).

10. Latham, V. M. J., Kislauskis, E. H., Singer, R. H. & Ross, A. F. Beta-actin mRNA localization is regulated by signal transduction mechanisms. *J. Cell Biol.* **126,** 1211–1219 (1994).

11. Yao, J., Sasaki, Y., Wen, Z., Bassell, G. J. & Zheng, J. Q. An essential role for beta-actin mRNA localization and translation in Ca2+-dependent growth cone guidance. *Nat. Neurosci.* **9,** 1265–1273 (2006).

12. Leung, K. M. & Holt, C. E. Live visualization of protein synthesis in axonal growth cones by

409 microinjection of photoconvertible Kaede into Xenopus embryos. *Nat. Protoc.* (2008).
410 doi:10.1038/nprot.2008.113

411 13. Eom, T., Antar, L. N., Singer, R. H. & Bassell, G. J. Localization of a beta-actin messenger
412 ribonucleoprotein complex with zipcode-binding protein modulates the density of dendritic
413 filopodia and filopodial synapses. *J. Neurosci.* **23,** 10433–44 (2003).

414 14. Kislauskis, E. H., Zhu, X. & Singer, R. H. Sequences responsible for intracellular localization of
415 beta-actin messenger RNA also affect cell phenotype. *J. Cell Biol.* **127,** 441–51 (1994).

416 15. Yisraeli, J. K. VICKZ proteins: a multi-talented family of regulatory RNA-binding proteins. *Biol.*
417 *Cell* **97,** 87–96 (2005).

418 16. Yoon, Y. J. *et al.* Glutamate-induced RNA localization and translation in neurons. *Proc. Natl.*
419 *Acad. Sci. U. S. A.* **113,** E6877–E6886 (2016).

420 17. Hüttelmaier, S., Zenklusen, D., Lederer, M. & Dictenberg, J. Spatial regulation of [beta]-actin
421 translation by Src-dependent phosphorylation of ZBP1 : Abstract : Nature. *Nature* (2005).
422 doi:10.1038/nature04115

423 18. Gilchrist, D. A., Fargo, D. C. & Adelman, K. Using ChIP-chip and ChIP-seq to study the
424 regulation of gene expression: Genome-wide localization studies reveal widespread regulation
425 of transcription elongation. *Methods* **48,** 398–408 (2009).

426 19. Hafner, M. *et al.* PAR-CliP--a method to identify transcriptome-wide the binding sites of RNA
427 binding proteins. *J. Vis. Exp.* 2–6 (2010). doi:10.3791/2034

428 20. Nicholson, C. O., Friedersdorf, M. & Keene, J. D. Quantifying RNA binding sites transcriptome-
429 wide using DO-RIP-seq. *RNA* **23,** 32–46 (2017).

430 21. Konig, J. *et al.* iCLIP - Transcriptome-wide Mapping of Protein-RNA Interactions with Individual
431 Nucleotide Resolution. *J. Vis. Exp.* (2011). doi:10.3791/2638

432 22. Zielinski, J. *et al.* In vivo identification of ribonucleoprotein-RNA interactions. *Proc. Natl. Acad.*
433 *Sci.* **103,** 1557–1562 (2006).

434 23. Rogell, B. *et al.* Specific RNP capture with antisense LNA/DNA mixmers. *RNA* **23,** 1290–1302
435 (2017).

436 24. Gaspar, I., Wippich, F. & Ephrussi, A. Enzymatic production of single-molecule FISH and RNA
437 capture probes. *RNA* **23,** 1582–1591 (2017).

438 25. Roux, K. J., Kim, D. I. & Burke, B. BioID: A screen for protein-protein interactions. *Curr. Protoc.*
439 *Protein Sci.* (2013). doi:10.1002/0471140864.ps1923s74

440 26. Kim, D. I. *et al.* Probing nuclear pore complex architecture with proximity-dependent
441 biotinylation. *Proc. Natl. Acad. Sci.* **111,** E2453–E2461 (2014).

442 27. Kim, D. I., Jensen, S. C. & Roux, K. J. in *Methods in molecular biology (Clifton, N.J.)* **1411,**
443 133–146 (2016).

444 28. Roux, K. J., Kim, D. I., Raida, M. & Burke, B. A promiscuous biotin ligase fusion protein
445 identifies proximal and interacting proteins in mammalian cells. *J. Cell Biol.* **196,** 801–10
446 (2012).

447 29. Ramanathan, M. *et al.* RNA–protein interaction detection in living cells. *Nat. Methods* **15,** 207–
448 212 (2018).

449 30. Bell, J. L. *et al.* Insulin-like growth factor 2 mRNA-binding proteins (IGF2BPs): Post-
450 transcriptional drivers of cancer progression? *Cellular and Molecular Life Sciences* **70,** 2657–
451 2675 (2013).

452 31. Ceci, M. *et al.* RACK1 is a ribosome scaffold protein for β-actin mRNA/ZBP1 complex. *PLoS*
453 *One* **7,** (2012).

454 32. Gu, W., Pan, F., Zhang, H., Bassell, G. J. & Singer, R. H. A predominantly nuclear protein
455 affecting cytoplasmic localization of β-actin mRNA in fibroblasts and neurons. *J. Cell Biol.* **156,**
456 41–51 (2002).

457 33. Itoh, M., Haga, I., Li, Q.-H. & Fujisawa, J. Identification of cellular mRNA targets for RNA-
458 binding protein Sam68. *Nucleic Acids Res.* **30,** 5452–64 (2002).

459 34. Klein, M. E., Younts, T. J., Castillo, P. E. & Jordan, B. A. RNA-binding protein Sam68 controls
460 synapse number and local -actin mRNA metabolism in dendrites. *Proc. Natl. Acad. Sci.* **110,**
461 3125–3130 (2013).

462 35. Castets, M. *et al.* FMRP interferes with the Rac1 pathway and controls actin cytoskeleton

463 dynamics in murine fibroblasts. *Hum. Mol. Genet.* **14,** 835–844 (2005).

464 36. Rackham, O. & Brown, C. M. Visualization of RNA–protein interactions in living cells: FMRP
465 and IMP1 interact on mRNAs. *EMBO J.* **23,** 3346–3355 (2004).

466 37. Chung, H.-J. *et al.* FBPs Are Calibrated Molecular Tools To Adjust Gene Expression. *Mol.*
467 *Cell. Biol.* **26,** 6584–6597 (2006).

468 38. Quinn, L. M. FUBP/KH domain proteins in transcription: Back to the future. *Transcription* **8,**
469 185–192 (2017).

470 39. Blichenberg, a *et al.* Identification of a cis-acting dendritic targeting element in MAP2 mRNAs.
471 *J. Neurosci.* **19,** 8818–8829 (1999).

472 40. Rehbein, M., Kindler, S., Horke, S. & Richter, D. Two trans-acting rat-brain proteins, MARTA1
473 and MARTA2, interact specifically with the dendritic targeting element in MAP2 mRNAs. *Mol.*
474 *Brain Res.* **79,** 192–201 (2000).

475 41. Peabody, D. S. The RNA binding site of bacteriophage MS2 coat protein. *Embo J* **12,** 595–600
476 (1993).

477 42. Park, H. Y. *et al.* Visualization of dynamics of single endogenous mRNA labeled in live mouse.
478 *Science (80-.).* **343,** 422–424 (2014).

479 43. Lawrence, J. B. & Singer, R. H. Intracellular localization of messenger RNAs for cytoskeletal
480 proteins. *Cell* **45,** 407–15 (1986).

481 44. Tyagi, S. & Alsmadi, O. Imaging native β-actin mRNA in motile fibroblasts. *Biophys. J.* **87,**
482 4153–4162 (2004).

483 45. Dormoy-Raclet, V. *et al.* The RNA-Binding Protein HuR Promotes Cell Migration and Cell
484 Invasion by Stabilizing the -actin mRNA in a U-Rich-Element-Dependent Manner. *Mol. Cell.*
485 *Biol.* **27,** 5365–5380 (2007).

486 46. Heraud-Farlow, J. E. & Kiebler, M. A. The multifunctional Staufen proteins: Conserved roles
487 from neurogenesis to synaptic plasticity. *Trends in Neurosciences* **37,** 470–479 (2014).

488 47. McDermott, S. M., Meignin, C., Rappsilber, J. & Davis, I. Drosophila Syncrip binds the gurken

mRNA localisation signal and regulates localised transcripts during axis specification. *Biol. Open* **1,** 488–497 (2012).

48. Zivraj, K. H. *et al.* The RNA-binding protein MARTA2 regulates dendritic targeting of MAP2 mRNAs in rat neurons. *J. Neurochem.* **124,** 670–684 (2013).

49. Lionnet, T. *et al.* A transgenic mouse for in vivo detection of endogenous labeled mRNA. *Nat. Methods* **8,** 165–170 (2011).

50. Gáspár, I., Sysoev, V., Komissarov, A. & Ephrussi, A. An RNA-binding atypical tropomyosin recruits kinesin-1 dynamically to oskar mRNPs. *EMBO J.* **36,** 319–333 (2017).

51. Eliscovich, C., Shenoy, S. M. & Singer, R. H. Imaging mRNA and protein interactions within neurons. *Proc. Natl. Acad. Sci.* **114,** E1875–E1884 (2017).

52. Park, H. Y., Trcek, T., Wells, A. L., Chao, J. A. & Singer, R. H. An Unbiased Analysis Method to Quantify mRNA Localization Reveals Its Correlation with Cell Motility. *Cell Rep.* **1,** 179–184 (2012).

53. Wu, B., Buxbaum, A. R., Katz, Z. B., Yoon, Y. J. & Singer, R. H. Quantifying Protein-mRNA Interactions in Single Live Cells. *Cell* **162,** 211–20 (2015).

54. Jønson, L. *et al.* Molecular composition of IMP1 ribonucleoprotein granules. *Mol. Cell. Proteomics* **6,** 798–811 (2007).

55. Mingle, L. A. *et al.* Localization of all seven messenger RNAs for the actin-polymerization nucleator Arp2/3 complex in the protrusions of fibroblasts. *J. Cell Sci.* **118,** 2425–2433 (2005).

56. Kim, H. H., Lee, S. J., Gardiner, A. S., Perrone-Bizzozero, N. I. & Yoo, S. Different motif requirements for the localization zipcode element of ??-actin mRNA binding by HuD and ZBP1. *Nucleic Acids Res.* **43,** (2015).

57. Farina, K. L., H??ttelmaier, S., Musunuru, K., Darnell, R. & Singer, R. H. Two ZBP1 KH domains facilitate ??-actin mRNA localization, granule formation, and cytoskeletal attachment. *J. Cell Biol.* **160,** 77–87 (2003).

58. Dominguez, D. *et al.* Sequence, Structure, and Context Preferences of Human RNA Binding Proteins. *Mol. Cell* **70,** 854–867.e9 (2018).

59. Bell, J. L. *et al.* Insulin-like growth factor 2 mRNA-binding proteins (IGF2BPs): post-transcriptional drivers of cancer progression? *Cell. Mol. Life Sci.* **70,** 2657–75 (2013).

60. Hollingworth, D. *et al.* KH domains with impaired nucleic acid binding as a tool for functional analysis. *Nucleic Acids Res.* **40,** 6873–86 (2012).

61. Stöhr, N. *et al.* IGF2BP1 promotes cell migration by regulating MK5 and PTEN signaling. *Genes Dev.* **26,** 176–89 (2012).

62. Roux, K. J. Marked by association: techniques for proximity-dependent labeling of proteins in eukaryotic cells. *Cell. Mol. Life Sci.* **70,** 3657–3664 (2013).

63. Schopp, I. M. *et al.* Split-BioID a conditional proteomics approach to monitor the composition of spatiotemporally defined protein complexes. *Nat. Commun.* **8,** 15690 (2017).

64. Rhee, H.-W. *et al.* Proteomic Mapping of Mitochondria in Living Cells via Spatially Restricted Enzymatic Tagging. *Science (80-.).* **339,** 1328–1331 (2013).

65. Fallini, C. *et al.* Dynamics of survival of motor neuron (SMN) protein interaction with the mRNA-binding protein IMP1 facilitates its trafficking into motor neuron axons. *Dev. Neurobiol.* **74,** (2014).

66. Donlin-Asp, P. G. *et al.* The Survival of Motor Neuron Protein Acts as a Molecular Chaperone for mRNP Assembly. *Cell Rep.* **18,** 1660–1673 (2017).

67. Latham, V. M., Yu, E. H., Tullio, A. N., Adelstein, R. S. & Singer, R. H. A Rho-dependent signaling pathway operating through myosin localizes beta-actin mRNA in fibroblasts. *Curr. Biol.* **11,** 1010–6 (2001).

68. Song, T. *et al.* Specific interaction of KIF11 with ZBP1 regulates the transport of β-actin mRNA and cell motility. *J. Cell Sci.* **128,** (2015).

69. Donnelly, C. J., Fainzilber, M. & Twiss, J. L. Subcellular Communication Through RNA Transport and Localized Protein Synthesis. *Traffic* **11,** 1498–1505 (2010).

70. Gáspár, I., Sysoev, V., Komissarov, A. & Ephrussi, A. An RNA-binding atypical tropomyosin recruits kinesin-1 dynamically to *oskar* mRNPs. *EMBO J.* (2017).

542 doi:10.15252/embj.201696038

543 71. Wickham, H. *Ggplot2*. *Elegant Graphics for Data Analysis* (2009). doi:10.1007/978-0-387-

544 98141-3

545

546 **FIGURES:**

547

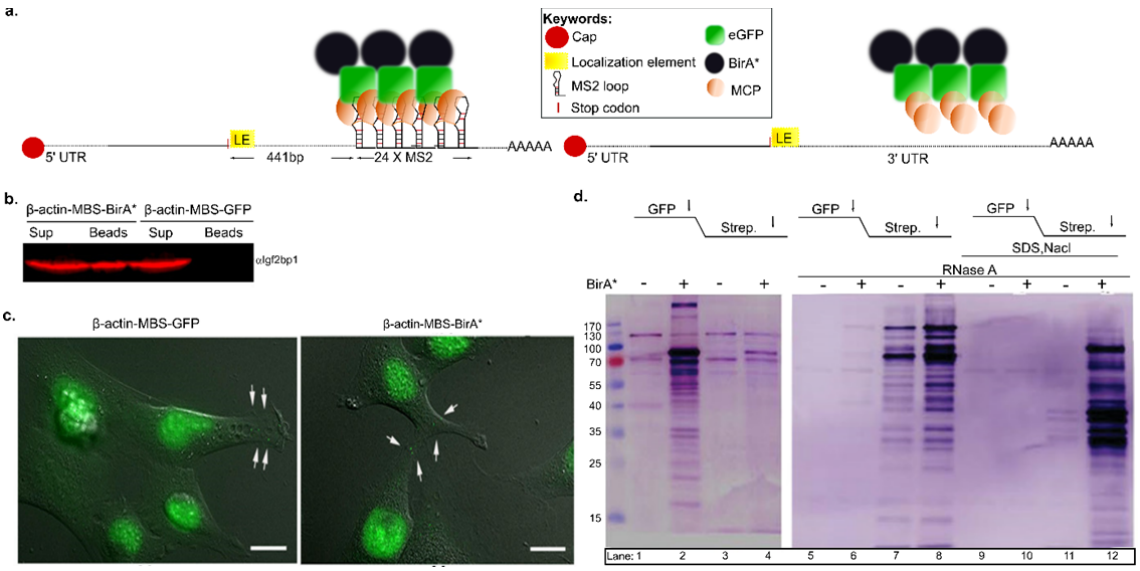

548
549

550

551 **Figure 1: RNA BioID to detect proteins interacting with localized β-actin RNA.**

552 (a) Schematic of the β-actin-MBS-BirA* and control constructs to detect β-actin mRNA associated proteins. The
553 24xMS2 loop (24MBS) array was integrated in the 3'UTR of the endogenous β-actin gene 441 bp downstream of
554 the stop codon. BirA* is targeted to 24MBS by fusing it to 2xMCP-eGFP (upper panel) Control cells expressed
555 2xMCP-eGFP-BirA* and β-actin mRNA lacking the MBS cassette (lower panel).

556 (b) Biotinylation of IGF2BP1 depends on MBS sites in β-actin. Following RNase A treatment, botinylated proteins
557 were affinity-purified with streptavidin-coated beads from cells expressing 2xMCP-eGFP-BirA* in the presence
558 (β-actin-24MBS) or absence (β-actin) of MCP binding sites (MBS). Presence of IGF2BP1 was probed by a
559 specific antibody in bead fraction (Beads) and supernatant (Sup).

560 (c) β-actin-MBS MEFs expressing 2xMCP-eGFP (left panel) or 2xMCP-eGFP-BirA* (right panel) form and
561 localize β-actin mRNP particles (arrows) after 24hr of serum starvation and 2 hr serum induction. The nuclear
562 accumulation of 2xMCP-eGFP or 2xMCP-eGFP-BirA* originates from a nuclear localization signal (NLS) at the
563 N-terminus of the fusion proteins. Bar: 10 μm.

564 (d) Specific enrichment of β-actin-MBS associated, biotinylated proteins are achieved by stringent conditions
565 during purification. Two consecutive affinity purifications (anti-GFP followed by streptavidin pulldown) were
566 performed. Western blots were stained for biotinylated proteins by streptavidin-alkaline peroxidase. Left panel:
567 The majority of the biotinylated proteins remain associated with 2xMCP-eGFP-BirA* in the GFP pulldown fraction
568 under low-stringency purification conditions (lane 2). Combination of treatment with RNaseA (lane 6 versus 8), or
569 0.5% SDS and 500 mM NaCl (lane 10 versus 12) leads to quantitative enrichment of biotinylated proteins by
570 streptavidin pulldown.

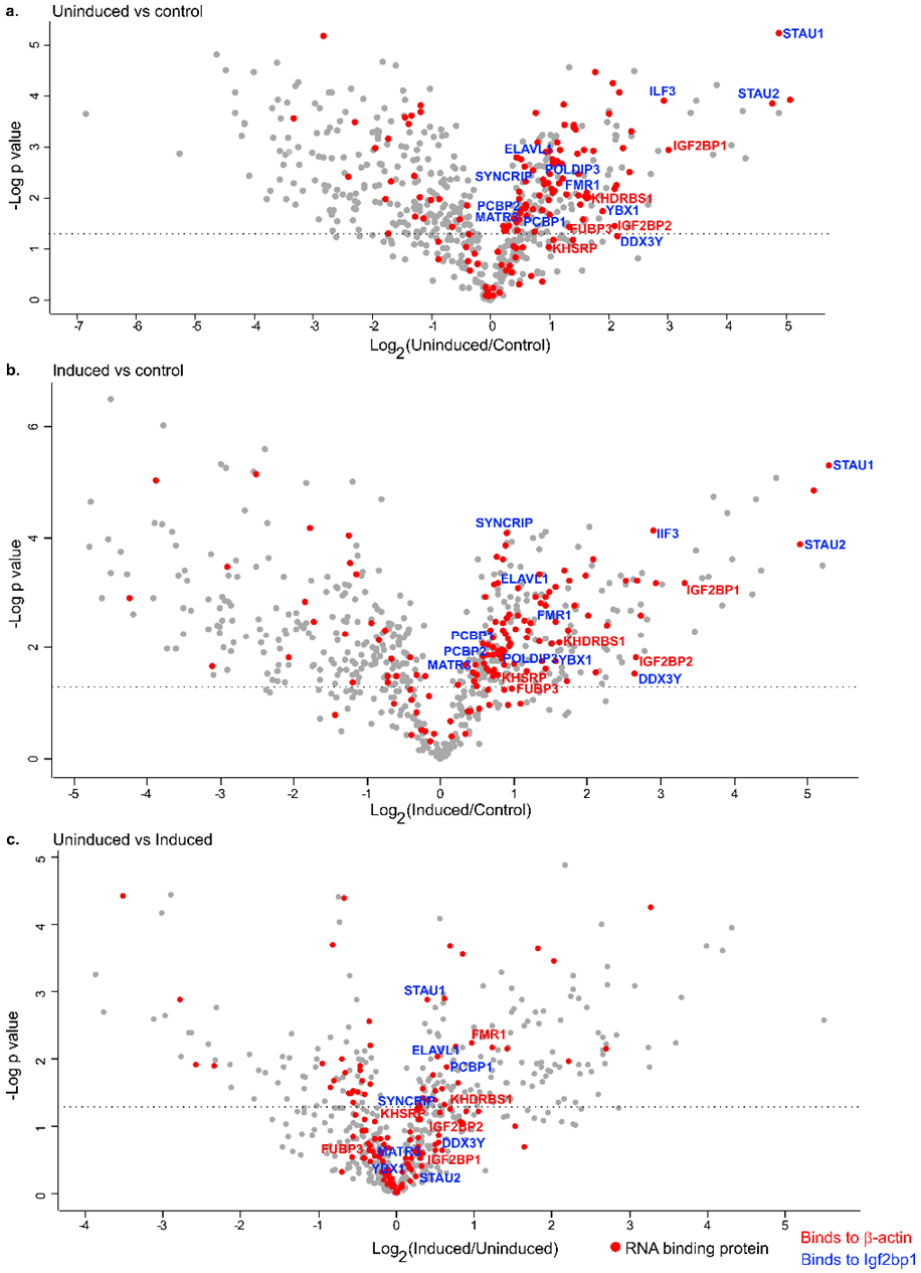

Figure 2: Enrichment of biotinylated proteins in control MEFs, or MEFs expressing β actin-MBS-BirA* under serum-induced or uninduced conditions.

Volcano plot representation of biotinylated proteins in

(a) uninduced MEFs compared to control MEFs,

(b) serum-induced MEFs compared to control MEFs.

(c) serum-induced MEFs compared to uninduced MEFs.

In the volcano plots, the X-axis represents log2 fold change in protein abundance and the Y-axis represents the –log10 p-value. Red circles are known RBPs identified by GO-molecular function analysis. Proteins names in red represent known β-actin mRNA interactors and proteins named in blue are RBPs known to bind to IGF2BP1. Dotted line indicates p = 0.05.

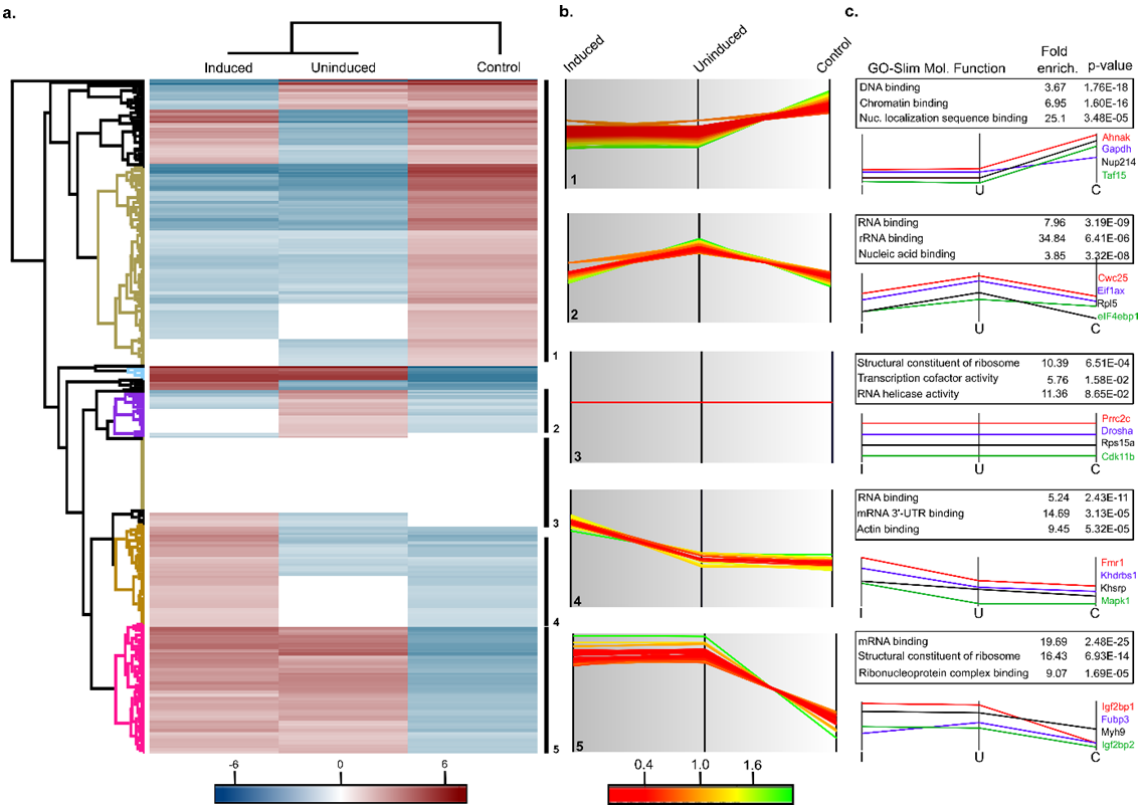

Figure 3: Cluster analysis of biotinylated proteins in control MEFs or MEFs expressing β-actin-MBS-BirA* under serum-induced or uninduced conditions.

(a) Hierarchical clustering of biotinylated proteins in serum-induced, uninduced β-actin-MBS-BirA* MEFs and control MEFs (lacking β-actin-MBS). Enrichment is indicated in red coloring, depletion in blue. Various clusters of protein groups are highlighted in the dendrogram.

(b) Profile plots of five selected clusters showing distinct enrichment patterns of biotinylated proteins: 1. Strongly enriched in control MEFs; 2. Enriched in β-actin-MBS-BirA* MEFs under uninduced condition; 3. Similar enrichment in all MEFs. 4. Enriched in β-actin-MBS-BirA* MEFs under serum-induced conditions; 5. Enriched in β-actin-MBS-BirA* MEFs under serum induced and uninduced conditions compared to the control MEFs. Degree of enrichment in each specific cluster is represented by coloring (green, more enriched, red, less enriched).

(c) Functional analysis of protein annotation terms results in multiple categories that are enriched in the selected clusters. GO-slim molecular function terms, the corresponding enrichment factor, and the p-value are shown in the table. Selected examples of proteins found in each cluster are depicted below the tables.

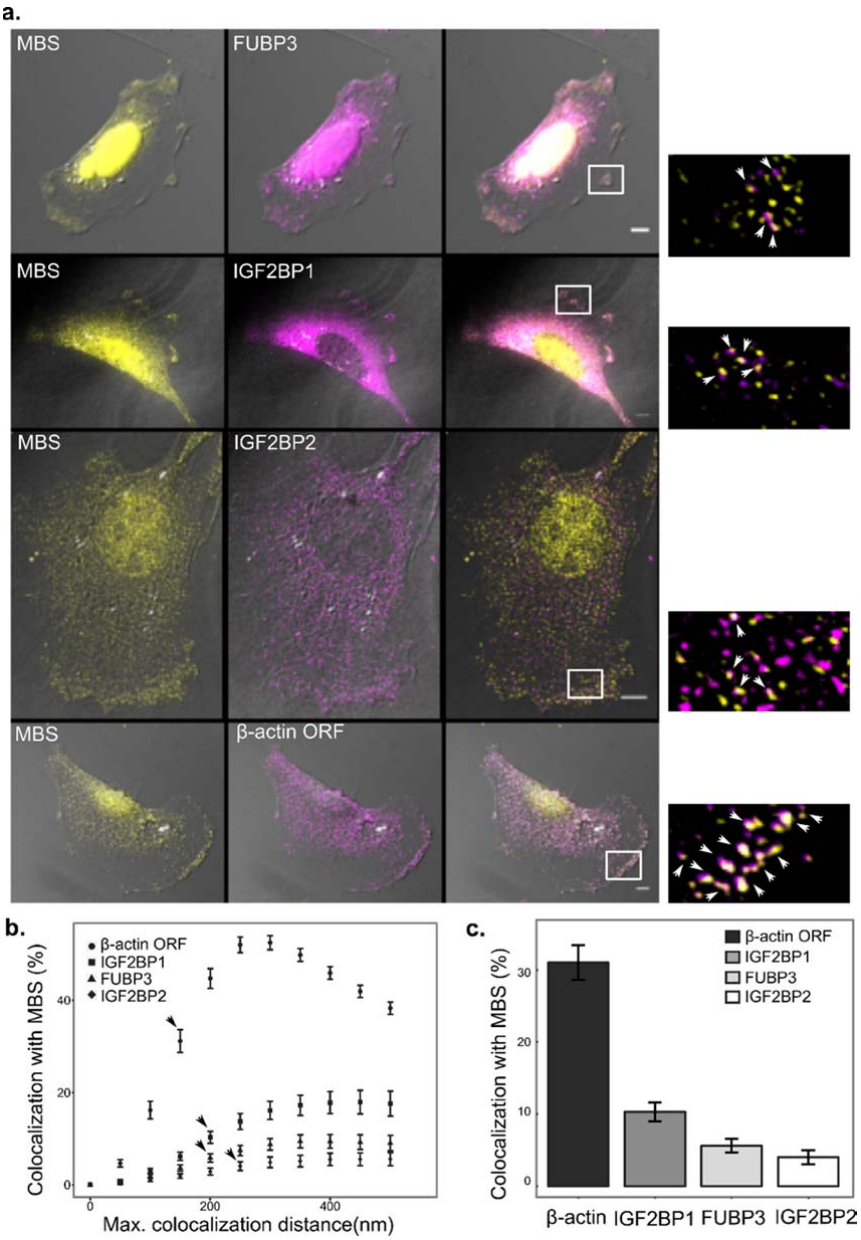

598

599 **Figure 4: Colocalization of IGF2BP1 and FUBP3 with β-actin-MBS mRNA.**

600 (a) Representative smFISH-immunofluorescence images in MEFs expressing β-actin-MBS. RNA is detected with
601 smFISH probes against MBS (yellow) or against β-actin ORF (magenta), proteins with antibodies against either
602 FUBP3, IGF2BP1, IGF2BP2 (magenta). Boxed areas indicate magnified regions. Arrows indicate colocalizing
603 objects. Scale bar represent 5 µm.

604 (b) Difference between observed and random estimated colocalization plotted as a function of maximal
605 colocalization distance. Arrows indicate the maximal colocalization distance chosen to analyze and compare the
606 ratio of colocalization presented in (c) (150 nm for β-actin ORF probes, 200 nm for IGF2BP1 and FUBP3 and 250
607 nm for IGF2BP2). This point was chosen as the midway between zero and the onset of the plateau which
608 represent the domination of random colocalization on the difference values. See Supplementary Figure S9 for
609 more data.

610 (c) Degree of colocalization of β-actin-MBS with β-actin ORF, IGF2BP1, FUBP3 or IGF2BP2. Histogram bars
611 represent the difference values at the maximal colocalization distance as indicated by the arrows in (b). Errors
612 bar represent 95% confidence interval.

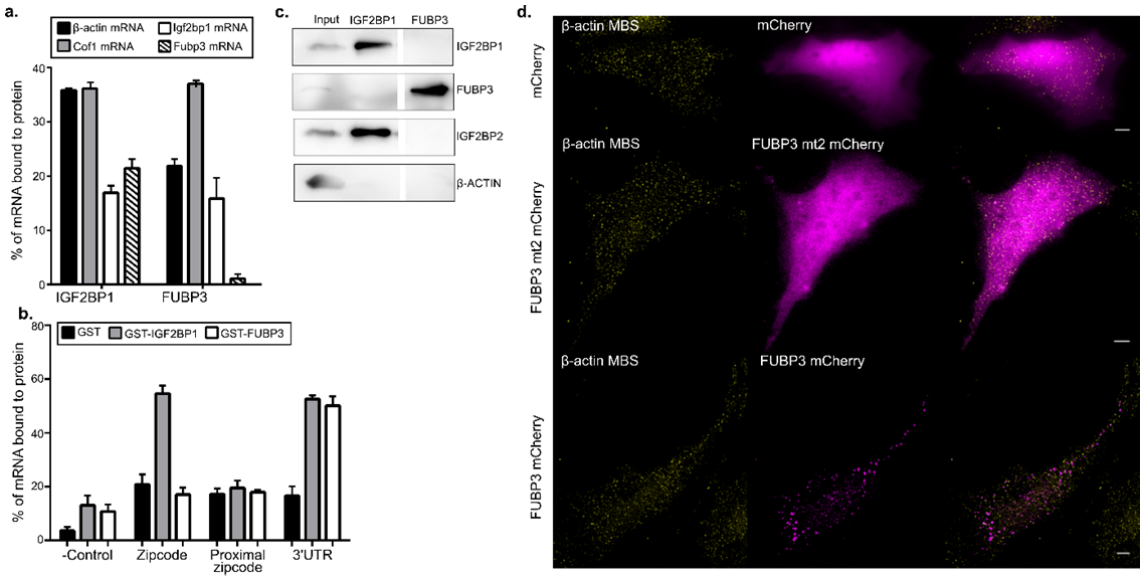

Figure 5: FUBP3 binds to β-actin 3'UTR.

a) Co-immunoprecipitation of selected mRNAs with IGF2BP1 and FUBP3. Bars represent percentage of input mRNA co-purifying with the indicated protein. IGF2BP1 binds to several endogenous mRNAs such as, Cofilin1, Igf2bp1 and Fubp3. FUBP3 binds to 23% of endogenous β-actin mRNA while IGF2BP1 was associated with 37% of endogenous β-actin mRNA. Error bars represents mean ± sem from three independent experiments.

(b) RNA pulldown of GST fusion proteins of IGF2BP1 and FUBP1. In vitro transcribed RNA fragments of β-actin (zipcode, proximal zipcode, full-length 3'UTR, and a zipcode mutant as negative control) were added to *E. coli* lysates with expressed GST or GST fusion proteins. Proteins and bound RNAs were isolated and bound RNA detected by quantitative RT-PCR. Bars represent percentage of input RNA. IGF2BP1 shows high affinity for the zipcode sequence whereas FUBP3 does not. Instead it binds to the 3'UTR. Error bars represents mean±sem from three independent experiments.

(c) Co-immunoprecipitation of FUBP3 and IGF2BP1. Immunoprecipitation was performed from wild type MEFs either with FUBP3 or IGF2BP1 specific antibodies. IGF2BP1 co-precipitates with IGF2BP2 but not with FUBP3. FUBP3 co-purifies neither IGF2BP1 nor IGF2BP2.

(d) RNA-binding domain KH2 is required for FUBP3 cytoplasmic granule formation. The conserved G-X-X-G motif of FUBP3 KH domains were individually mutated into G-D-D-G and wildtype and mutant proteins expressed in MEFs as mCherry fusion. Live cell imaging shows that wild type FUBP3-mCherry forms cytoplasmic granules whereas a KH2 mutant (FUBP3 mt2) is evenly distributed in the cytoplasm like the control mCherry protein. Scale bar represent 5 μm.

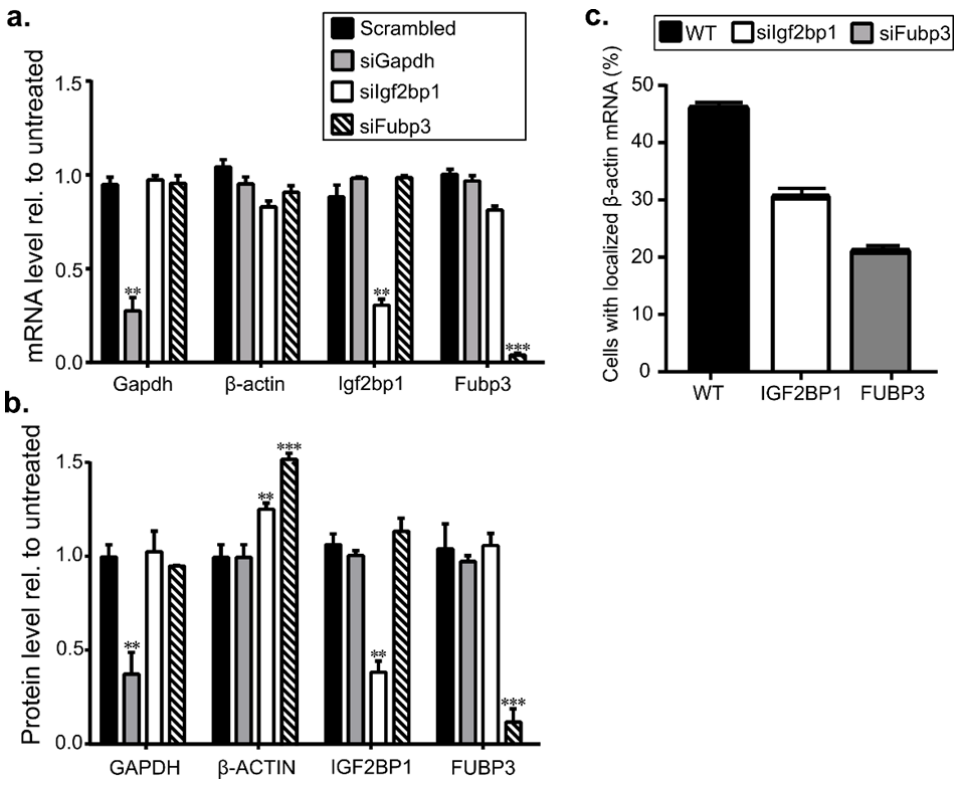

Figure 6: Downregulation of Fubp3 affects β-actin mRNA localization.

(a)-(c) Cells were treated for 72 hrs with scrambled siRNAs or siRNAs against Gapdh, Fubp3 or Igf2bp1.

(a) Quantitative RT-PCR analysis of Gapdh, Igf2bp1, β-actin, Fubp3 levels in knockdown cells. mRNAs in untreated cells was used to normalize.

(b) Western blot analysis of GAPDH, IGF2BP1, β-ACTIN, FUBP3 levels in knockdown cells. Protein levels in untreated cells were used as normalization control.

(c) Percentage of cells with localized β-actin mRNA in wild type MEFs and upon depletion of Igf2bp1 or Fubp3. Total number of cells analyzed is 562 in wild type, 241 in Igf2bp1 knockdown MEFs and 343 in Fubp3 knockdown MEFs. Localization of β-actin-MBS mRNA to the cell protrusions was manually scored by smFISH against β-actin MBS.

Statistical significance of each dataset was determined by Student's t-test; *P < 0.05; ***P < 0.001. Error bars represents mean±sem from 3 independent experiments.